

**IMECE2005-80508**

## **A COMPARATIVE, EXPERIMENTAL STUDY OF MODEL SUITABILITY TO DESCRIBE VEHICLE ROLLOVER DYNAMICS FOR CONTROL DESIGN**

**John T. Cameron**

Department of Mechanical and Nuclear Engineering  
The Pennsylvania State University  
318 Leonhard Building  
University Park, PA 16802

**Sean Brennan**

Department of Mechanical and Nuclear Engineering  
The Pennsylvania State University  
318 Leonhard Building  
University Park, PA 16802  
sbrennan@psu.mne.edu

### **ABSTRACT**

This work presents results of an initial investigation into models and control strategies suitable to prevent vehicle rollover due to untripped driving maneuvers. Outside of industry, the study of vehicle rollover inclusive of both experimental validation and practical controller design is limited. The researcher interested in initiating study on rollover dynamics and control is left with the challenging task of identifying suitable vehicle models from the literature, comparing these models with experimental results, and determining suitable parameters for the models. This work addresses these issues via experimental testing of published models. Parameter estimation data based on model fits is presented, with commentary given on the validity of different methods. Experimental results are then presented and compared to the output predicted by the various models in both the time and frequency domain in order to provide a foundation for future work.

### **INTRODUCTION**

Vehicle accidents are the single largest cause of fatalities for males 44 years and under and for females 34 years and under [1]. The societal impact of vehicle safety is clearer when considering the number of life-years lost: For all people who die under the age of 65, accidental death due to motor vehicle accidents claim over 1.2 million potential life years [2]. There are more potential life years lost to this age group due to automotive accidents than any other cause [2]. These deaths are sudden, and most often strike when a person is at the peak of both their professional and personal/family life. While vehicle rollover is involved in only 2.5% of the 11 million accidents a year, it accounts for approximately 20% of all fatalities [3]. That means approximately 250,000 potential life years are lost per year due to vehicle rollover.

The National Highway Traffic Safety Administration (NHTSA) is charged with ensuring vehicle safety, and recognizing the increasing statistics of rollover, formally adopted the concept of the static stability factor (SSF) in January of 2001. The SSF is a relatively simple metric that is intended to give consumers a qualitative assessment of a vehicles resistance to rollover. It is a ratio of track width divided by two times the height of the vehicle CG. A higher number is intended to indicate better "rollover stability." For current production vehicles, the highest value of the SSF is approximately 1.45 [4].

One problem with the SSF is that it is purely a steady-state measure and gives little indication of the transient response to a given steering input. Consideration of transient response is especially important when noting that NHTSA has never tested a vehicle that will rollover under steady-state turning situations [5]. The obvious need for transient vehicle handling data is highlighted by the 2000 Congressional mandate known as the TREAD Act, which includes a provision for NHTSA to develop a test program designed to evaluate a vehicles rollover propensity under dynamic conditions by November 2002. Additionally, a report by the National Academy of Science published in February of 2002 further asserted the need for NHTSA to develop a dynamic rollover testing program to accompany the SSF. These transient tests are now used in addition with the SSF in the "star" rating system.

As a result of ongoing experimental research, NHTSA has developed a number of transient maneuvers that, given a high enough speed, induce vehicle rollover [6, 7]. Some vehicles will evidently rollover in a transient maneuver despite not rolling over at steady state, which implies that a resonant mode exists in the roll response. This resonance will occur at different frequencies for different vehicles, yet NHTSA has chosen only a few representative transient maneuvers to test all vehicles. Because it is unlikely that all vehicles are excited equally at

their resonant mode by the same maneuvers, a more careful consideration of roll resonance is needed. In particular, experimental tests might require customized maneuvers for each vehicle model that most excite that vehicle's resonant frequency. Finding this frequency clearly requires a model-based approach.

In addition to finding dynamic models of vehicle rollover, this study is further focused on finding dynamic models that are well suited to the design and implementation of online, real-time controllers. These controllers are increasingly used to prevent the onset of rollover. A goal of this work is to understand the linear vehicle dynamics prior to the point where tire saturation nonlinearities become significant, therefore only linear models are considered. Additionally, one would like to avoid performing dangerous transient maneuvers in an academic environment, therefore the models must be able to predict vehicle motion without dynamic fitting, e.g. using parameters easily measured offline or from stable driving. Suitability for controller synthesis is determined by a number of factors including the accuracy of the model for moderate steering inputs (e.g. linear tire behavior), the order and simplicity of the dynamic model, the number of parameters entering the model.

The remainder of the paper is organized as follows: Section 2 presents the results of the literature survey performed by the authors. Section 3 presents the models chosen for this study. Experimental results and comparisons with model predictions are presented in Section 4. Finally, Section 5 presents preliminary conclusions from this ongoing study.

## NOMENCLATURE

$U_x$	Longitudinal velocity (body-fixed frame)
$U_y$	Lateral velocity (body-fixed frame)
$m$	Vehicle mass
$m_s$	Vehicle sprung mass
$I_{zz}$	Inertia about the vertical (Z) axis
$I_{xx}$	Inertia about the roll (X) axis
$I_{yy}$	Inertia about the pitch (Y) axis
$I_{xz}$	Inertia product
$l_f$	Front-axle-to-CG distance
$l_r$	Rear-axle-to-CG distance
$L$	Track of vehicle ( $l_f + l_r$ )
$t$	Width of vehicle
$K_\phi$	Effective roll stiffness of the suspension
$D_\phi$	Effective roll damping of the suspension
$h$	CG height
$\alpha_f$	Slip angle of the front tires
$\alpha_r$	Slip angle of the rear tires
$\beta$	Slip angle of the vehicle body
$C_f$	Front cornering stiffness
$C_r$	Rear cornering stiffness
$\delta_f$	Front steering angle

## 2. LITERATURE SURVEY RESULTS

An extensive, but not exhaustive, search of recent literature found twenty-three unique vehicle models that include a mathematical description of roll dynamics. Of these, only three

will be utilized in this study [8-10]. The reasoning used to narrow down the number of models under consideration is discussed below.

It is noted that many publications include models focused on trailer dynamics [11, 12], only examined suspension dynamics, ignored longitudinal and lateral motion [13], sought to only investigate the effect of lateral acceleration on vehicle rollover [14], simply estimated roll with a correcting term [15, 16], or dealt with tripped rollovers [17, 18]. These models are excluded from consideration.

Another significant portion of the models found were discounted because there was simply not enough information given in the paper to recreate the simulations or derivations. For instance, [19-22] did not provide the equations of motion used for reported simulations and experimental comparisons. Others simply did not define all of the symbols used in their model [23] or provide sufficient detail to recreate equation derivations [24].

Additional factors narrowing model selection included the use of an overly complex model unsuitable for control synthesis. These include models derived from kinematic software packages that generate equations of motion that are too complex (high order) to be suitable for feedback control design [25, 26]. Other models included parameters that were either difficult to measure or whose physical meaning is unclear [27, 28]. Because the goal of this study is to develop models based on first-principles without the need for fitting under rollover-inducing situations, these models were abandoned.

Finally there was the category of models that, although the equations of motion were presented, a number of errors existed such that they were not reproducible in simulation [29-31]. In the case of [29, 30], the same model was presented in state-space form [30] and in transfer function form [29]. However, parameters were different between the two papers, with neither set seeming to reproduce published results. The state-space representation proved to be open-loop unstable.

For these reasons, this study will focus on models based upon those derived in [8-10]. These three models still require information obtained through experimental measurement [9], but the physical meaning of these parameters is clear, allows offline estimation, or can be estimated with moderate maneuvers.

A distinguishing feature of this study is the nature of the parameter fitting. One method is assume a given mathematical model and then vary all of the parameters in until an optimal fit with experimental data is obtained. While this may provide a "good" fit, the drawback of this approach is that the parameters can quickly lose their physical significance. For instance, allowing wide variation in the mass and length parameters of a vehicle,  $m$ ,  $l_f$ , and  $l_r$ , might indeed provide an improved fit but detracts from the physical meaning implied by these parameters.

This study seeks to avoid such instances by (1) not assuming that any mathematical models are inherently suitable, (2) directly measuring as many vehicle parameters as possible offline, or obtaining the parameters from an externally validated source such as NHTSA, and (3) only allowing variation in those parameters that have either not been measured or possess a high degree of uncertainty. Such an approach helps to allow comparison of underlying models (and their assumptions), and ensures that the predictive capabilities

of a given model are based on the physical parameters of the vehicle to which it is applied. The intent of these constraints are to facilitate prediction of the roll response of many vehicles without the need to fit a model to each of them individually.

### 3. VEHICLE MODELS

To emphasize the similarity between the models used in this study, each is presented and derived in similar fashion using similar state definitions and coordinate systems. All numerical representations follow the standard SAE right-handed sign convention shown in Fig 1. In some cases, this sign convention differs from the original publications.

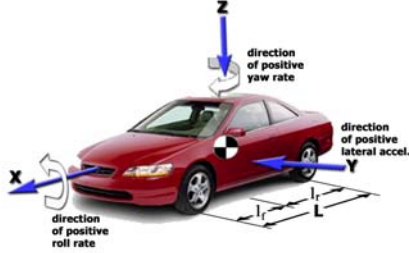


Figure 1: SAE Coordinate System

For brevity, some details of each model derivation have been omitted from this work. Each of the models is presented in a compact symbolic notation of the form:

$$M_i \cdot \ddot{q} + D_i \cdot \dot{q} + K_i \cdot q = F_i \cdot u_f \quad (1)$$

where  $i$  denotes the model number (1 to 4 for this study), and

$$q = \{y \ \psi \ \phi\}^T \quad (2)$$

denotes the state vector, which is lateral position, yaw angle, and roll angle respectively. The general form described by Eq. (1) allows for an intuitive term-by-term comparison between different models. Further details on the derivation of each model can be found in the original publications.

#### Model 1- 2DOF Model Assuming No Roll Dynamics

The planar dynamics of the 3DOF models will be compared to a 2DOF model commonly found in literature. Typically referred to as the “bicycle model”, it assumes a single track vehicle that only exhibits lateral and yaw dynamics. This model is commonly used in studies on tire slip estimation [32], vehicle body slip estimation [33], automated steering controllers [34-36], and vehicle stability [37, 38] to name a few.

While it does not have any roll dynamics, the bicycle model is considered here as a reference and because it is known to provide a reasonable match to experimental data for both lateral acceleration and yaw rate dynamics for maneuvers that are not very aggressive. Further, the parameters defined for the bicycle model are also found in all of the 3DOF models used in this study, and hence this relatively simple model can be used to determine a number of the parameters used in the other 3DOF models. Finally, it allows for a comparison between the effect of including roll on the lateral and yaw-rate dynamics.

The equations of motion may be derived from a simple examination of the lateral dynamics of the vehicle. This results in the non-linear equations:

$$\begin{bmatrix} \sum F_y \\ \sum M_z \\ \sum M_x \end{bmatrix} = \begin{bmatrix} -m \cdot U \cdot \varpi \cdot \cos(\beta) \\ -I_{zz} \cdot \ddot{\psi} \\ 0 \end{bmatrix} \quad (3)$$

where:

$$\varpi = (\dot{\beta} + \dot{\psi}) \quad (4)$$

$$\beta = \tan^{-1} \left( \frac{v_y}{v_x} \right) \approx \frac{V}{U} \quad (5)$$

In determining the external forces and moments acting on the vehicle, the first assumption is that the lateral forces acting on each tire is directly proportional to the slip of that tire and that both tires on an axle share the same forces. This leads to the equations:

$$F_f = C_f \alpha_f = C_f \left( \delta_f - \beta - \frac{l_f}{U} r \right) \quad (6)$$

$$F_r = C_r \alpha_r = C_r \left( -\beta + \frac{l_r}{U} r \right) \quad (7)$$

where:

$$\alpha_{f,1} = \tan^{-1} \left( \frac{-U\beta - l_f r}{U} \right) + \delta_f = \delta_f - \beta - \frac{l_f r}{U} \quad (8)$$

$$\alpha_{r,1} = \tan^{-1} \left( \frac{l_r r - U\beta}{U} \right) \cong \frac{l_r r}{U} - \beta \quad (9)$$

The simplifying assumptions made for Eqs. (8) and (9) are that the slip angles are small enough to allow a linear approximation and that right- and left-side differences in tire forces are negligible. Longitudinal forces acting upon the tires are assumed to be zero, and longitudinal velocity,  $U$ , is assumed to be constant.

Consideration of the forces acting on the vehicles tires, the external forces and moments sum to be:

$$\begin{bmatrix} \sum F_y \\ \sum M_z \\ \sum M_x \end{bmatrix} = \begin{bmatrix} 2F_f + 2F_r \\ 2l_f F_f - 2l_r F_r \\ 0 \end{bmatrix} \quad (10)$$

Linearizing Eq. (3) and placing it in the form specified by Eq. (1) results in:

$$M_1 = \begin{bmatrix} -m & 0 & 0 \\ 0 & -I_{zz} & 0 \\ 0 & 0 & 0 \end{bmatrix} \quad (11)$$

$$D_1 = \begin{bmatrix} 0 & 0 & 0 \\ 0 & 0 & 0 \\ 0 & 0 & 0 \end{bmatrix} \quad (12)$$

$$K_1 = \begin{bmatrix} 0 & -mU & 0 \\ 0 & 0 & 0 \\ 0 & 0 & 0 \end{bmatrix} \quad (13)$$

$$F_1 = \begin{bmatrix} 2 & 2 \\ 2l_f & -2l_r \\ 0 & 0 \end{bmatrix} \quad (14)$$

#### Model 2 - 3DOF Model Assuming Existence of Sprung Mass and No X-Z Planar Symmetry

The following model will be based upon the derivation presented by Mammar et. al. [39]. The model presented here will differ in that the vehicle equations will be derived in a body-fixed frame instead of being referenced to a global frame (otherwise known as error coordinates). It will also conform to

the standard SAE coordinate system noted earlier. By applying basic kinematics, the authors obtain non-linear equations of motion are obtained:

$$\begin{bmatrix} \sum F_y \\ \sum M_z \\ \sum M_x \end{bmatrix} = \begin{bmatrix} -m \cdot U \cdot \sigma \cdot c(\beta) - m_s \cdot h \cdot \dot{\psi}^2 \cdot s(\phi) + m_s \cdot h \cdot (\dot{\phi}^2 \cdot s(\phi) - \ddot{\phi} \cdot c(\phi)) \\ -I_{zz} \cdot \ddot{\psi} \cdot c(\phi) - I_{xz} \cdot \dot{\phi} + I_{y1} \cdot \dot{\phi} \cdot \dot{\psi} \cdot s(\phi) + I_{xz} \cdot \dot{\psi}^2 \cdot s(\phi) \cdot c(\phi) \\ I_{xx} \cdot \ddot{\phi} + I_{xz} \cdot \ddot{\psi} + I_{y2} \cdot \dot{\psi}^2 \cdot s(\phi) \cdot c(\phi) + m_s \cdot h \cdot U \cdot \sigma \cdot c(\beta) \cdot c(\phi) + m \cdot h^2 \cdot \dot{\psi}^2 \cdot c^2(\phi) \end{bmatrix} \quad (15)$$

where:

$$I_{y1} = (I_{zz} + I_{xx} - I_{yy})$$

$$I_{y2} = (I_{zz} - I_{yy}) \quad (16)$$

and:

$$c(x) = \cos(x) \quad (17)$$

$$s(x) = \sin(x)$$

Applying the same small-angle assumptions that lead to Eq. (8) and Eq (9), the external forces acting on the vehicle are:

$$\begin{bmatrix} \sum F_y \\ \sum M_z \\ \sum M_x \end{bmatrix} = \begin{bmatrix} 2 \cdot F_f + 2 \cdot F_r \\ 2 \cdot l_f \cdot F_f - 2 \cdot l_r \cdot F_r \\ -(K_\phi \cdot \phi + D_\phi \cdot \dot{\phi}) + m_s \cdot g \cdot h \cdot \phi \end{bmatrix} \quad (18)$$

Finally, by equating the internal and external force-moment equations, combined with a small angle assumption and neglecting all terms of powers greater than one by assuming them to be small compared to the remaining terms, the linear equations are obtained. Following the general form specified by Eq. (1), these are given by:

$$M_2 = \begin{bmatrix} -m & 0 & -m_s h \\ 0 & -I_{zz} & -I_{xz} \\ m_s h & I_{xz} & I_{xx} \end{bmatrix} \quad (19)$$

$$D_2 = \begin{bmatrix} 0 & -mU & 0 \\ 0 & 0 & 0 \\ 0 & m_s h U & D_\phi \end{bmatrix} \quad (20)$$

$$K_2 = \begin{bmatrix} 0 & 0 & 0 \\ 0 & 0 & 0 \\ 0 & 0 & K_\phi - m_s g h \end{bmatrix} \quad (21)$$

$$F_2 = \begin{bmatrix} 2 & 2 \\ 2l_f & -2l_r \\ 0 & 0 \end{bmatrix} \quad (22)$$

### Model 3 - 3DOF Model Assuming Existence of Sprung Mass, X-Z Planar Symmetry, and Roll Steer Influence

Kim and Park present a 3 DOF model that is derived in body-fixed coordinates and describes the vehicle's lateral velocity, yaw rate, roll rate, and roll angle [9]. The only notable differences between the derivation presented here and that of the original work is that each tire is analyzed individually in this work, a different sign is assumed of the cornering stiffness values to maintain consistency with SAE convention, and the SAE coordinate system is used.

The non-linear equations of motion are:

$$\begin{bmatrix} \sum F_y \\ \sum M_z \\ \sum M_x \end{bmatrix} = \begin{bmatrix} -m \cdot U \cdot \sigma \cdot c(\beta) - m_s \cdot h \cdot \dot{\psi}^2 \cdot s(\phi) + m_s \cdot h \cdot (\dot{\phi}^2 \cdot s(\phi) - \ddot{\phi} \cdot c(\phi)) \\ -I_{zz} \cdot \ddot{\psi} \cdot c(\phi) + I_{y1} \cdot \dot{\phi} \cdot \dot{\psi} \cdot s(\phi) \\ I_{xx} \cdot \ddot{\phi} + I_{y2} \cdot \dot{\psi}^2 \cdot s(\phi) \cdot c(\phi) + m_s \cdot h \cdot U \cdot \sigma \cdot c(\beta) \cdot c(\phi) + m \cdot h^2 \cdot \dot{\psi}^2 \cdot c^2(\phi) \end{bmatrix} \quad (23)$$

A notable difference in Model 3 versus the previous model is that Model 3 assumes that the vehicle is symmetric about the x-z plane, thus making  $I_{xz}$  zero and eliminating all cross terms.

Although the external forces acting upon the vehicle are identical to Eq (9) in form, the front and rear slip angles are redefined as:

$$\alpha_{f,2} = \delta_f + \frac{\partial \alpha_f^*}{\partial \phi} \phi - \beta - \frac{l_f}{U} r \quad (24)$$

$$\alpha_{r,2} = \frac{\partial \alpha_r^*}{\partial \phi} \phi - \beta + \frac{l_r}{U} r \quad (25)$$

to include camber effects due to roll.

Note the appearance of a partial derivative term in Eq. (24) and Eq. (25). A star is included in the notation of these terms to indicate that they refer to the influence of the vehicle's roll angle on the slip angle of the vehicle. This effect is commonly known as "roll steer" and is usually assumed to be a constant value when the amount of tire slip is small. Specified in [9], the magnitude of the coefficient for the front tires was 0.2, and -0.2 for the rear tires, and will be utilized in this study as well. However, it was found by the authors that alteration of this parameter had little effect on the models behavior.

Placing the equations of motion into the form specified by Eq. (1), the mass, damping, stiffness, and force matrices are:

$$M_3 = \begin{bmatrix} -m & 0 & -m_s h \\ 0 & -I_{zz} & 0 \\ m_s h & 0 & I_{xx} \end{bmatrix} \quad (26)$$

$$D_3 = \begin{bmatrix} 0 & -mU & 0 \\ 0 & 0 & 0 \\ 0 & m_s h U & D_\phi \end{bmatrix} \quad (27)$$

$$K_3 = \begin{bmatrix} 0 & 0 & 0 \\ 0 & 0 & 0 \\ 0 & 0 & K_\phi \end{bmatrix} \quad (28)$$

$$F_3 = \begin{bmatrix} 2 & 2 \\ 2l_f & -2l_r \\ 0 & 0 \end{bmatrix} \quad (29)$$

### Model 4 - 3DOF Model Assuming Sprung Mass Suspended on a Massless Frame and X-Z Planar Symmetry

The next model presented is based on the model derived by Carlson et. al [8]. Both the coordinate system and the notation have been changed from the original publication to coincide with those used in this work. Additionally, longitudinal tire forces will not be considered as a result of the assumptions of constant velocity and that the tires are rolling without slipping.

In this formulation, the sprung mass is equal to the total mass of the vehicle. Applying the modified kinematics formulas yields the non-linear equations:

$$\begin{bmatrix} \sum F_y \\ \sum M_z \\ \sum M_x \end{bmatrix} = \begin{bmatrix} -m \cdot U \cdot \sigma \cdot c(\beta) - m \cdot h \cdot \dot{\psi}^2 \cdot s(\phi) + m \cdot h \cdot (\dot{\phi}^2 \cdot s(\phi) - \ddot{\phi} \cdot c(\phi)) \\ -I_{zz} \cdot \ddot{\psi} \cdot c(\phi) + I_{y1} \cdot \dot{\phi} \cdot \dot{\psi} \cdot s(\phi) \\ I_{xx} \cdot \ddot{\phi} + I_{y2} \cdot \dot{\psi}^2 \cdot s(\phi) \cdot c(\phi) + m \cdot h \cdot U \cdot \sigma \cdot c(\beta) \cdot c(\phi) + m \cdot h^2 \cdot \dot{\psi}^2 \cdot c^2(\phi) \end{bmatrix} \quad (30)$$

Another distinction of Model 4 is in the formulation of the external forces acting on the vehicle. These equate to:

$$\begin{bmatrix} \sum F_y \\ \sum M_z \\ \sum M_x \end{bmatrix} = \begin{bmatrix} 2 \cdot F_f + 2 \cdot F_r \\ 2 \cdot l_f \cdot F_f - 2 \cdot l_r \cdot F_r \\ -(K_\phi \cdot \phi + D_\phi \cdot \dot{\phi}) + m \cdot g \cdot h \cdot \phi + 2 \cdot h \cdot F_f + 2 \cdot h \cdot F_r \end{bmatrix} \quad (31)$$

Further insight into the change in the external roll moment is obtained by examining the linear equations of motion. Linearizing Eq. (30) and placing them into the form specified by Eq. (1) gives:

$$M_4 = \begin{bmatrix} -m & 0 & -mh \\ 0 & -I_{zz} & 0 \\ 0 & 0 & I_{xx} \end{bmatrix} \quad (32)$$

$$D_4 = \begin{bmatrix} 0 & -mU & 0 \\ 0 & 0 & 0 \\ 0 & 0 & D_\phi \end{bmatrix} \quad (33)$$

$$K_4 = \begin{bmatrix} 0 & 0 & 0 \\ 0 & 0 & 0 \\ 0 & 0 & K_\phi - mgh \end{bmatrix} \quad (34)$$

$$F_4 = \begin{bmatrix} 2 & 2 \\ 2l_f & -2l_r \\ 2h & 2h \end{bmatrix} \quad (35)$$

with the external forces  $F_f$  and  $F_r$  following the formulation of Model 1.

#### General Discussion of Model Differences

Examination of the equations of motion of all of the models in this study reveals the similarities between Model 1 and Models 2, 3, and 4. It is therefore reasonable to expect that the lateral acceleration and yaw rate dynamics of the four models might be similar as well.

Model 2 is the most complex roll model presented in this study. This complexity comes from the fact that the vehicle is assumed to be asymmetric about the x-z plane. When compared with Model 2, Models 3 and 4 have less cross-coupling of the acceleration terms as a result of the assumption of symmetry about the x-z plane.

Model 3 has slightly higher roll stiffness than Models 2 and 4 which can be attributed to the omission of the downward acceleration of the vehicle sprung mass center when perturbed from its equilibrium position. This results in Model 2 having a roll stiffness that is approximately 1.2% greater than what is found in Models 2 and 4 (see values in Sec. 4). Such a small influence of the term  $m_s g h$  likely justifies omission from the formulation for this reason.

A primary difference between Model 4 versus Models 2 and 3 is that the total mass of the vehicle is assumed to be supported by the suspension, with the frame being assumed massless. This assumption causes Model 4 to be the simplest parametrically (i.e. requires the least number of parameters). Another distinguishing feature that simplifies the notation of Model 4 in the form described by Eq. (1) is that the term  $mh$  that should appear in the lower left hand corner of the mass matrix,  $M_i$ . Also, the term  $mhU$  that appears in the lower middle of the damping matrix,  $D_i$ , on Models 2 and 3 is replaced by the external forces acting on the tires. The force resulting from the lateral acceleration of the mass center may be equated to the external tire forces from a simple force balance when viewing the vehicle as an inverted pendulum.

## 4. EXPERIMENTAL RESULTS AND COMPARISONS

### Description of Parameters

Table 1 presents the parameter values used including brief descriptions as to how those values were obtained for the experimental vehicle of this study. For  $I_{zz}$ ,  $C_f$ , and  $C_r$ , the description ‘model fit’ refers to parametric fits obtained from a series of time-domain and frequency domain experiments. These experiments were divided into two steps: determination of the understeer gradient, and model matching in the frequency domain. Details on these experiments are given below.

Those parameters listed with ‘NHTSA database’ as a source were obtained by inspection of the National Highway Traffic Safety Administration database [40]. All experiments were performed on a 5-door 1992 Mercury Tracer whose data is listed in this database (these values match within a few percent of more crude measurement methods available to the authors). Additionally, care was taken to ensure that the experiments were conducted at relatively low accelerations. Others have noted that if the lateral acceleration remains below 0.4 g’s, that assumptions of linearity in the vehicle dynamics appear quite reasonable [41], so this limit is enforced for all testing.

Variable	Value	Units	Uncertainty	How it was determined
$m$	1030	kg	5%	Measured
$W_f$	6339	N	5%	Measured
$W_r$	3781	N	5%	Measured
$m_s$	825	kg	5%	Model Fit <sup>2</sup>
$I_{zz}$	1850	kg-m <sup>2</sup>	5%	Model Fit <sup>1</sup>
$I_{yy}$	1705	kg-m <sup>2</sup>	5%	NHTSA database
$I_{xx}$	375	kg-m <sup>2</sup>	5%	NHTSA database
$I_{xz}$	72	kg-m <sup>2</sup>	5%	NHTSA database
$l_f$	0.93	m	5%	Measured <sup>1</sup>
$l_r$	1.56	m	5%	Measured <sup>1</sup>
$l$	1.4	m	5%	Measured <sup>1</sup>
$h$	0.52	m	5%	NHTSA database
$K_\phi$	53000	N*m/rad	10%	Model Fit <sup>2</sup>
$D_\phi$	7000	N*m*s/rad <sup>2</sup>	10%	Model Fit <sup>2</sup>
$C_f$	-45500	N/rad	10%	Model Fit <sup>2</sup>
$C_r$	-76650	N/rad	10%	Model Fit <sup>2</sup>
$K_{us}$	0.045	rad/g	5%	Experimentally Determined

<sup>1</sup> - Indicates that the value is within 5% of the NHTSA database value.

<sup>2</sup> - Indicates that the value is not published in a readily available public database

**Table 1:** Parameter values

### Determination of Understeer Gradient

The understeer gradient of a vehicle characterizes how a vehicle’s response to a steering input changes with respect to global lateral acceleration. Most production vehicles are characterized as “understeer”, meaning that the faster the steady-state velocity through a constant-radius turn, the greater is the required steady-state steering angle needed to make that turn. The understeer gradient may be determined from a plot of steering angle vs. lateral acceleration and fitting a line to the data. The slope of the fit line is the understeer gradient. This steady-state relationship is defined explicitly as:

$$\delta_f = \frac{L}{R} + K_{us} \cdot a_y \quad (36)$$

where  $L/R$  is the steering angle required to make a given turn as lateral acceleration approaches zero,  $K_{us}$  is the understeer gradient and  $a_y$  is the lateral acceleration of the vehicle in the

global (earth-fixed) frame. Further information and equation derivations may be found in a number of sources including [42, 43].

An important consequence of the understeer gradient is that it may be related to the mass of the vehicle and the cornering stiffness'. It may be shown that this relationship is:

$$K_{us} = \frac{W_r}{2 \cdot C_r} - \frac{W_f}{2 \cdot C_f} \quad (37)$$

where  $W_f$  is the weight of the front of the vehicle and  $W_r$  is the weight of the rear.

In order to determine the understeer gradient, the test vehicle was driven at a constant 6.7, 8.9, and 11.2m/s around a 30.5m radius turn. The yaw rate was measured and used to determine the lateral acceleration using the relationship:

$$a_y = U \cdot r \quad (38)$$

For each test, the vehicle was driven around the test circle for approximately sixty seconds, the recorded steering angle and yaw rate were averaged, and the constant term  $L/R$  was subtracted from the steering angle to provide the data points. The results are shown below in Fig. 2.

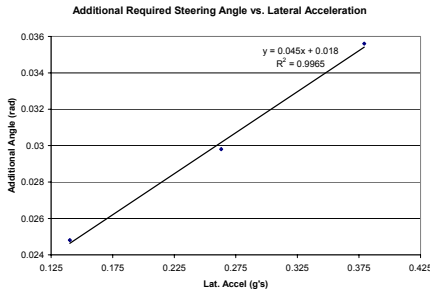


**Figure 2:** Steering Angle vs. Lateral Acceleration

The results shown in Fig. 2 suggest that it is reasonable to assume that the measured understeer gradient of 0.045 has a high degree of accuracy. Using this value in conjunction with Eq. (37) a relationship between the front and rear cornering stiffness values is obtained relating front to rear cornering stiffnesses in terms of understeer gradient and vehicle mass. This relationship is enforced later in estimating cornering stiffnesses.

#### Frequency Response Tests – Bicycle Model Fit

In order to determine the validity of the preceding models, the models are compared in the frequency domain. The frequency response test involved inputting sinusoidal steering inputs at frequencies varying between 0.33 Hz and 3.33 Hz. Frequencies below 0.33 Hz were omitted due to limited space on the test track, and higher frequencies were omitted as a result of physical limitations of the driver. To maintain constant frequency and phase, the sinusoidal steering input was synchronized to a digital metronome. Additionally, witness marks on the steering wheel were used to ensure consistency in amplitude.

The dynamic sinusoidal response of the vehicle was recorded in the yaw, roll, and lateral acceleration states. A sinusoid was then fit to the recorded steering input by a nonlinear fitting routine that minimized sum-of-squares error between measured data and a best-fit sine wave. From the best-fit sine wave, the frequency, amplitude, and phase angle of the

input signal was obtained. A similar fit was then performed on the output data; however the output frequency was not allowed to vary but was fixed at the input frequency. With sinusoid fits for both the input and output signals, the frequency response was readily determined.

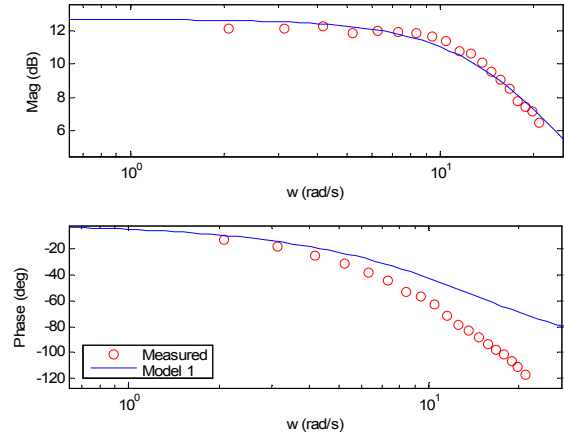


**Figure 3:** Measured frequency response from Steering Angle to Yaw Rate at 16 m/s, no tire lag, Model 1 fit

Examination of the phase lag observed in the frequency response data showed that no set of cornering stiffness parameters could be found that caused the models to match the measured data exactly. This was especially true in the yaw response where the predicted yaw rate had significantly less lag than the measured data revealed. It has been shown in literature [44] that a lag effect occurs in tire force generation, an effect known as tire lag. Tire lag is also known to be velocity dependent, i.e. the vehicle must travel a certain distance in order for the tire forces to reach steady state.

The tire-lag phenomenon is commonly modeled as a first-order system with zero steady-state gain. Such a model is introduced in this study using a model described by:

$$\frac{\delta_f^*}{\delta_f} = \frac{1}{\tau \cdot s + 1} \quad (36)$$

with  $\delta_f$  being the steering input at the tire generated by the driver and  $\delta_f^*$  being the effective steering input entering the bicycle model. Here  $\tau$  defined as:

$$\tau = \frac{D_{ss}}{U} \quad (37)$$

where  $D_{ss}$  is the distance required for the tire to reach steady-state. Note that  $\tau$  is inversely proportional to forward velocity, and hence more noticeable for the relatively low-speed driving studied in this work (~30 mph). Typical values in the literature are between 0.5m and 1m [44]. By varying the tire-lag dynamics of the bicycle model (Model 1), it was found that a value of 0.6m fit the measured data from the vehicle quite well in phase (Fig. 4).

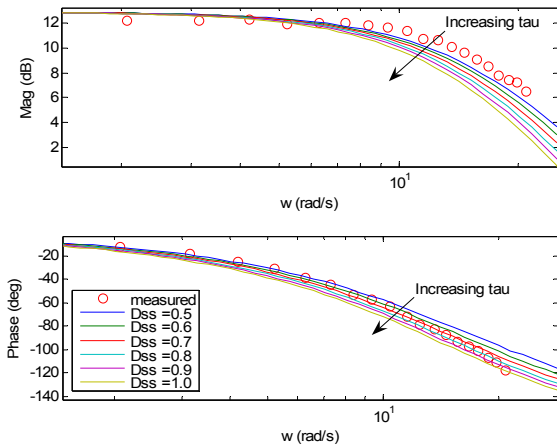


**Figure 4:** Frequency response from Steering Angle to Yaw Rate, with bicycle model fit varying tire lag

*Frequency Response Tests – Roll Model Fit*

The two parameters that remained to be estimated for model fit were  $K_\phi$  and  $D_\phi$ . To accomplish this, these parameters were varied manually until the models best matched the frequency response data. The resulting frequency-domain fits are seen in Figures 5-7, where each shows experimental data in circles and model prediction in lines for the four models of this study.

In examination of Figure 5, the model predictions do not match the data until the input frequencies are high. This is likely due to the influence of gravity on sensor measurements due to the roll of the vehicle. As the vehicle rolls, an accelerometer mounted on the sprung mass does as well. In so doing it no longer remains planar and therefore the acceleration measurements are corrupted by gravity. Whether this roll is induced by road bank angle as in [45] or by vehicle dynamics, the effect is the same. The authors were unable to correct for neither the roll angle of the vehicle nor the road bank angle as the test vehicle currently lacks the sensing capabilities to determine absolute roll angle. At present only roll *rate* may be recorded with current sensors. However the vehicle is in the process of being instrumented with an inertial measurement unit capable of providing roll and pitch measurements.

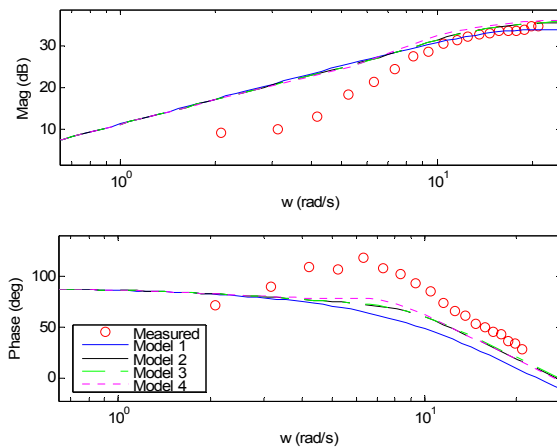


**Figure 5:** Frequency Response, Steering Input to Lateral Acceleration, Mercury Tracer, 16.5 m/s

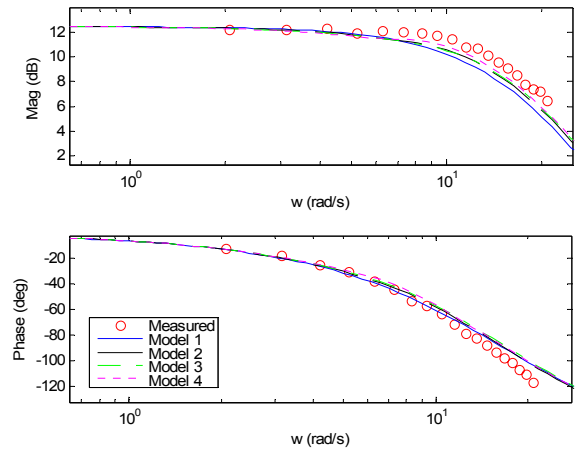


**Figure 6:** Frequency Response, Steering Input to Yaw Rate, Mercury Tracer, 16.5 m/s

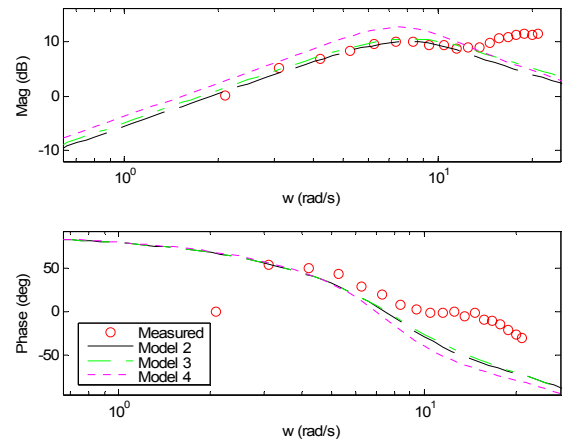


**Figure 7:** Frequency Response, Steering Input to Roll Rate, Mercury Tracer, 16.5 m/s

At low frequencies, the magnitude of the steering input was high in order to ensure the excitation of the plant dynamics. However, as the speed increased, the magnitude of the steering input was decreased in order to ensure that the performance would remain within linear bounds. While the increased magnitude of the input at lower frequencies ensured excitation of the lateral dynamics, it also likely resulted in a higher roll angle of the vehicle. It therefore is reasonable to assume that there was a higher degree of cross coupling between the lateral acceleration measurements and gravity at low frequencies than there was at higher frequencies.

Models 2-4 show similar behavior to Model 1 in both the lateral acceleration response and the yaw rate response. This is to be expected as the planar dynamics of roll models are derived from slight modifications of Model 1.

Finally, while model matching of the yaw response is excellent for all of the models, it does not fit as well in the roll rate response. The measured data for the magnitude plot begins to diverge at approximately 13 rad/s, while the measured phase diverges from the predicted values at approximately 9.5 rad/s. The effect has been shown to be repeatable, and is believed to be a problem in data collection and not with the individual models. A separate validation with an independent sensor system based on an inertial measurement unit is ongoing to determine the cause of this mismatch.

### Time Response Tests – Step Response

In order to obtain a more intuitive understanding of the model fit obtained by the frequency response tests, time response data were taken (Fig. 8). The first maneuver performed was a step response. The vehicle was driven forward at a constant speed of 8.9 m/s for an unspecified period of time. A step input of approximately 0.095 rad front wheel angle was then executed and the resulting vehicle response was recorded. Note that due to the current limitations in data collection the roll rate data was obtained during a separate trial, and thus has a slightly different steering command associated with it.

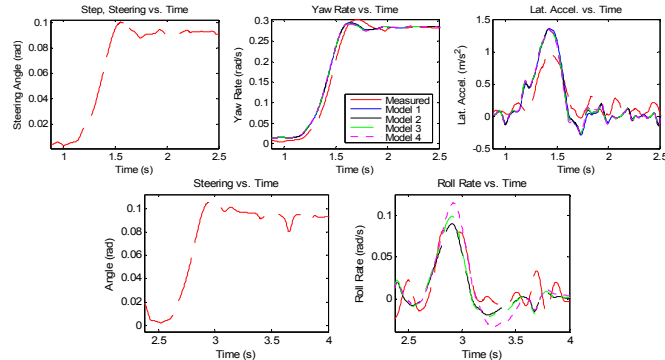


**Figure 8:** Step Response, Mercury Tracer, 8.9 m/s, Frequency Domain Fit Parameters

The predicted yaw response of all of the models is identical and matches the measured response well. The lateral acceleration response is also similar to the trends seen in the frequency response data, with all of the models producing a response of greater magnitude than the measured response. Some phase error can also be seen in lateral acceleration. The roll rate matches reasonably well, with the measured magnitude being slightly higher than the predicted values. The response of each model is similar, with Model 1 and 2 being nearly identical, and Model 3 appearing to be slightly less damped.

### Time Response Tests – Lane Change Maneuver

The next time-domain experiment was a lane change maneuver whereby the vehicle moved from the right lane to the left lane, and then back to the right lane (Fig. 9). To conduct this test, the vehicle was brought up to a constant speed of 17.8 m/s and was made to follow a reference line specifying the maneuver painted on the test track surface. The results from the lane change maneuver were similar to those from the step response maneuver.

The yaw response again matches well. The roll rate response is also reasonable for all of the models, with Model 3 again appearing to be less damped than Models 1 and 2. This is likely due to the decoupling of the yaw dynamics from the roll dynamics.

There is poor model matching observed again in lateral acceleration, and is far more evident with the lane change maneuver. Much like the frequency response data for this state, there is a mismatch in both the magnitude and phase of the data. As stated previously, this is likely due to influence of

gravity on the lateral accelerometer as a result of vehicle roll angle.

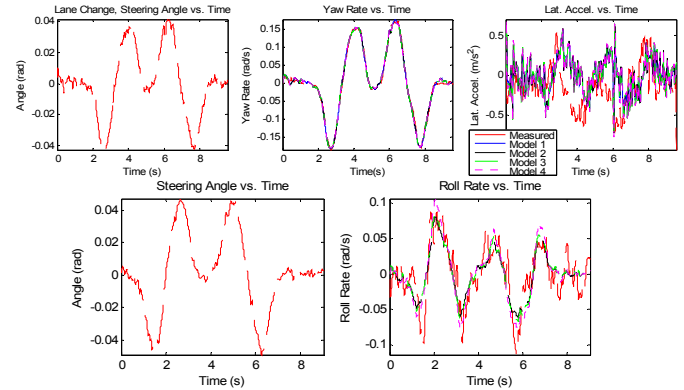


**Figure 9:** Lane Change, Mercury Tracer, 17.8 m/s, Frequency Domain Fit Parameters

### Time Response Tests – Model Fitting in the Time Domain

In the previous tests, it was shown that the time response data agreed with the findings of the frequency response data. Such an observation is expected, as the frequency domain represents the response of a plant to the complete range of inputs that it will encounter. However, many (if not most) vehicle chassis dynamic models are fit in the time domain. The question as to whether model fitting in the time domain gives a better fit than model fitting in the frequency domain was then posed.

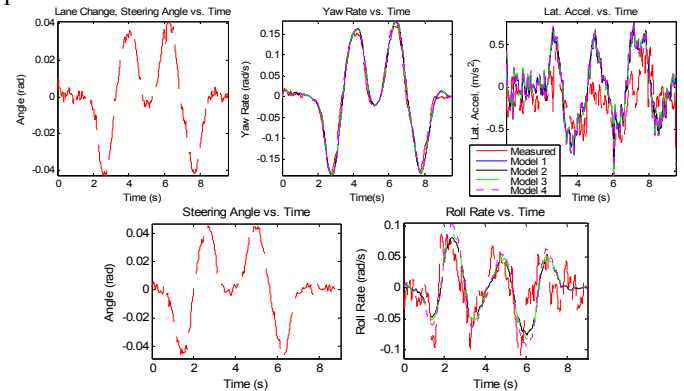


**Figure 10:** Lane Change, Mercury Tracer, 17.8 m/s, Time Domain Fit Parameters

In an attempt to answer this, the models were fit to the time response data shown in Fig. 10 and 11. These lane-change and step-input tests were chosen as they are commonly used to validate models in literature [20, 24, 31, 46-48]. At first glance, it would appear as if the parameters found are excellent matches comparable to frequency domain fits of Fig. 5-7 (whose time-domain fits are shown in Figs. 8 and 9). However, the model parameters identified in the time domain show poor matching in the frequency domain. Fig. 12-14 shows poor model matching in all of the states. This suggests a serious shortcoming of using time response data for model validation, as it might appear that not all of the input frequencies are excited in a single maneuver. It is unclear as yet whether time-domain signals intentionally made rich in frequency content, e.g. chirp inputs, work better. Again, these tests are ongoing.

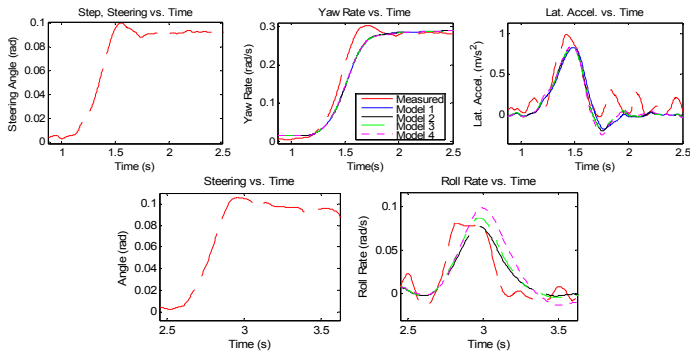


**Figure 11:** Step Response, Mercury Tracer, 8.9 m/s, Time Domain Fit Parameters

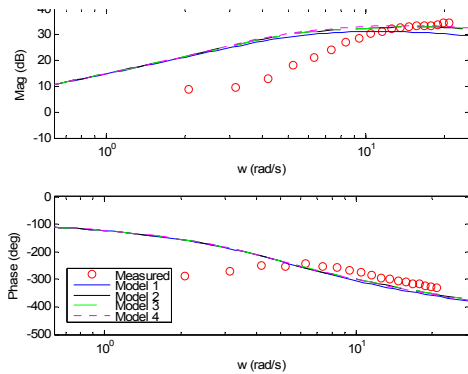


**Figure 12:** Frequency Response, Steering Input to Lateral Acceleration, Mercury Tracer, 16.5 m/s, Time Domain Fit Parameters

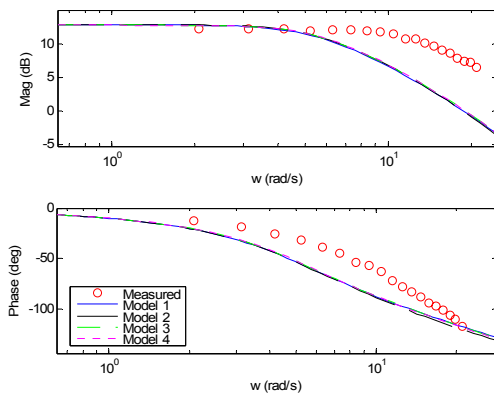


**Figure 13:** Frequency Response, Steering Input to Yaw Rate, Mercury Tracer, 16.5 m/s, Time Domain Fit Parameters

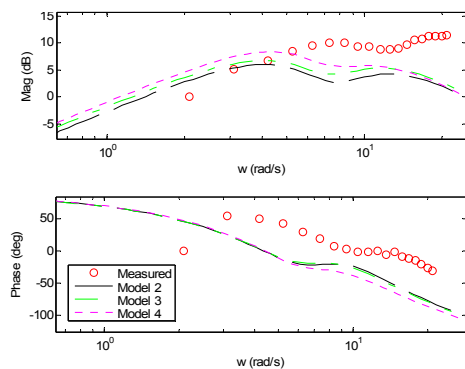


**Figure 14:** Frequency Response, Steering Input to Roll Rate, Mercury Tracer, 16.5 m/s, Time Domain Fit Parameters

## 5. CONCLUSIONS

A review of literature pertaining to the study of vehicle rollover has been performed and preliminary results shown in this work show a number of similarities between the models. However, this work also illustrates a number of problems associated with combining experimental and theoretical vehicle studies to validate and compare vehicle roll models, namely how to perform parameter fitting and discerning between fits on one state while mismatching in another. Although care was taken to carefully measure each physical parameter within the models, no model was found to be fully satisfactory in its accuracy to simultaneously predict the frequency-response of vehicle roll rate, vehicle yaw rate, and vehicle lateral acceleration.

Experimental results indicate that some models might appear to be a slightly better match than others, but that model-to-model differences are largely secondary to questions of whether fits should be obtained in time or frequency domains. The results indicate that in the absence of frequency response data, extra care must be taken when attempting to determine vehicle parameters against time response data since excitation may not be clear, even with step-response inputs. Future work will examine the use of other time response maneuvers such as the chirp response and the standard NHTSA maneuvers to determine the reliability of model fitting against these when compared to model fitting in the frequency domain.

Further work is currently under way to better verify vehicle parameters and to obtain improved models of vehicle behavior. One evident shortcoming in the approach used thus far is the requirement that all of the models be linear. Herein lies a significant difficulty in model-based rollover prediction and model-based controller synthesis to prevent vehicle rollover: while linearity greatly simplifies controller design, the limit handling maneuvers that ultimately induce rollover nearly always involve large tire forces and tire saturation. However, prior to examining non-linear models and control schemes, it is important to fully understand and control a vehicles dynamics in the linear range. Research is ongoing to better understand linear control techniques with the hope they will prevent the vehicle from ever entering the non-linear region.

## ACKNOWLEDGMENTS

The authors would like to acknowledge the assistance of Vishisht Gupta who assisted in the experiments performed in this work.

## REFERENCES

- [1] "Web-based Injury Statistics Query and Reporting System (WISQARS): Leading Causes of Death Reports, 1999 - 2002," vol. 2005. Atlanta, Georgia: The Center for Disease Control (CDC), 2002.
- [2] "Web-based Injury Statistics Query and Reporting System (WISQARS): Years of Potential Life Lost (YPLL) Reports, 1999 - 2002," vol. 2005. Atlanta, Georgia: The Center for Disease Control (CDC), 2002.
- [3] "Traffic Safety Facts 2003 - Final Report," U.S. Department of Transportation: National Highway Traffic and Safety Board 2004.
- [4] A. Y. Lee, "Coordinated Control of Steering and Anti-Roll Bars to Alter Vehicle Rollover Tendencies," *Journal of Dynamic Systems, Measurement, and Control*, vol. 124, pp. 127, 2002.
- [5] United States Department of Transportation, "An Experimental Examination of Selected Maneuvers That May Induce On-Road, Untripped Light Vehicle Rollover – Phase I-A of NHTSA's 1997-1998

- Vehicle Rollover Research Program," National Highway Traffic Safety Administration (NHTSA) HS 359 807, August 2001.
- [6] United States Department of Transportation, "An Experimental Examination of Selected Maneuvers That May Induce On-Road Untripped, Light Vehicle Rollover - Phase II of NHTSA's 1997-1998 Vehicle Rollover Research Program," National Highway Traffic Safety Administration (NHTSA) HS 808 977, July 1999.
- [7] United States Department of Transportation, "A Comprehensive Experimental Examination of Selected Maneuvers That May Induce On-Road, Untripped, Light Vehicle Rollover - Phase IV of NHTSA's Light Vehicle Rollover Research Program," National Highway Traffic Safety Administration HS 809 513, October 2002.
- [8] C. R. Carlson and J. C. Gerdes, "Optimal Rollover Prevention with Steer-by-Wire and Differential Braking," presented at Proceedings of IMECCHE, Washington D.C., 2003.
- [9] H.-J. Kim and Y.-P. Park, "Investigation of robust roll motion control considering varying speed and actuator dynamics," *Mechatronics*, 2003.
- [10] S. Mammari, "Speed Scheduled Vehicle Lateral Control," presented at Proceedings of the 1999 IEEE/IEEE/JSAI International Conference on Intelligent Transportation Systems, 1999.
- [11] D. Hyun, R. Langari, and J. Ochoa, "Vehicle Modeling and Prediction of Rollover Stability Threshold for Tractor-Semitrailers," presented at Proceedings of the 5th International Symposium on Advanced Vehicle Control (AVEC), Ann Arbor, Michigan, 2000.
- [12] V. Krishnaswami, "A Regularization Approach to Robust Variable Structure Observer Design Applied to Vehicle Parameter and State Estimation," presented at Proceedings of the 1998 American Control Conference, Philadelphia, Pennsylvania, 1998.
- [13] S. Ikenaga, F. L. Lewis, J. Campos, and L. Davis, "Active Suspension Control of Ground Vehicle based on a Full-Vehicle Model," presented at Proceedings of the 2000 American Control Conference, Chicago, Illinois, 2000.
- [14] S. Kueperkoch, J. Ahmed, A. Kojic, and J.-P. Hathout, "Novel Vehicle Stability Control Using Steer-By-Wire and Independent Four Wheel Torque Distribution," presented at Proceedings of the 2003 ASME International Mechanical Engineering Congress, Washington D.C., 2003.
- [15] R. Fenton, G. Melocik, and K. Olson, "On the steering of automated vehicles: Theory and experiment," *IEEE Transactions on Automatic Control*, vol. 21, pp. 306-315, 1976.
- [16] D. E. Williams and W. M. Haddad, "Nonlinear control of roll moment distribution to influence vehicle yaw characteristics," *IEEE Transactions on Control Systems Technology*, vol. 3, pp. 110-116, 1995.
- [17] R. Eger, "Rollover Simulations Based on a Nonlinear Model," *Society of Automotive Engineers*, vol. 1321, pp. 1-7, 1998.
- [18] R. Eger and U. Kiencke, "Modeling of rollover sequences," *Control Engineering Practice*, vol. 11, pp. 209-216, 2003.
- [19] J. Darling and L. R. Hickson, "Experimental study of a prototype active anti-roll suspension system," *Vehicle System Dynamics*, vol. 29, pp. 309-329, 1998.
- [20] S.-W. Oh, H.-C. Chae, S.-C. Yun, and C.-S. Han, "The Design of a Controller for the Steer-by-Wire System," *JSME International Journal, Series C*, vol. 47, pp. 896-907, 2004.
- [21] N. Rosam and J. Darling, "Development and simulation of a novel roll control system for the Interconnected Hydragas(R) Suspension," *Vehicle System Dynamics*, vol. 27, pp. 1-18, 1997.
- [22] T. J. Wielenga, "A Method For Reducing On-Road Rollovers Anti-Rollover Braking," vol. (none), (none), Ed., (none) ed. Detroit, Michigan: (none), 1999, pp. 87-98.
- [23] W. Manning, D. Crolla, M. Brown, and M. Selby, "Coordination of Chassis Control Systems for Vehicle Motion Control," presented at Proceedings of the 5th International Symposium on Advanced Vehicle Control (AVEC), Ann Arbor, Michigan, 2000.
- [24] K. Kitajima and H. Peng, "Control for Integrated Side-Slip, Roll, and Yaw Controls for Ground Vehicles," presented at Proceedings of the 5th International Symposium on Advanced Vehicle Control (AVEC), Ann Arbor, Michigan, 2000.
- [25] D. J. Cole, "Evaluation of design alternatives for roll-control of road vehicles," presented at Proceedings of the 5th International Symposium on Advanced Vehicle Control (AVEC), Ann Arbor, Michigan, 2000.
- [26] J. K. Sprague and S.-P. Liu, "Automated Stability Analysis of a Vehicle in Combined Pitch and Roll," presented at Proceedings of the 2002 ASME International Mechanical Engineering Congress and Exposition (IMECE), New Orleans, Louisiana, 2002.
- [27] B.-C. Chen and H. Peng, "Differential Braking Based Rollover Prevention for Sport Utility Vehicles with HIL Evaluations," *Vehicle System Dynamics*, vol. 36, pp. 359-389, 2001.
- [28] R. S. Sharp and D. Pan, "On the design of an active roll control system for a luxury car," *Proceedings of the Institution of Mechanical Engineers, Part D (Journal of Automobile Engineering)*, vol. 207, pp. 275-284, 1993.
- [29] K. T. Feng, Han-ShueTan, and M. Tomizuka, "Decoupling Steering Control for Vehicles Using Dynamic Look-Ahead Scheme," presented at Proceedings of the 5th International Symposium on Advanced Vehicle Control (AVEC), Ann Arbor, Michigan, 2000.
- [30] K.-T. Feng, H.-S. Tan, and M. Tomizuka, "Automatic Steering Control of Vehicle Lateral Motion with the Effect of Roll Dynamics," presented at Proceedings of the 1998 American Control Conference, Philadelphia, Pennsylvania, 1998.
- [31] S. Takano, M. Nagai, T. Taniguchi, and T. Hatano, "Study on a vehicle dynamics model for improving roll stability," *Japanese Society of Automotive Engineers Review*, vol. 24, pp. 149-156, 2003.
- [32] S. Saraf and M. Tomizuka, "Slip Angle Estimation for Vehicles on Automated Highways," presented at Proceedings of the 1997 American Control Conference, Albuquerque, New Mexico, 1997.
- [33] D. M. Bevly, R. Sheridan, and J. C. Gerdes, "Integrating INS Sensors with GPS Velocity Measurements for Continuous Estimation of Vehicle Sideslip and Tire Cornering Stiffness," presented at Proceedings of the 2001 American Control Conference, Arlington, Virginia, 2001.
- [34] J. Ackermann, W. Sienel, and R. Steinhauser, "Robust automatic steering of a bus," presented at Proceedings of the Second European Control Conference (ECC), Groningen, The Netherlands, 1993.
- [35] S. Mammari and V. B. Baghdassarian, "Two-degree-of-freedom Formulation of Vehicle Handling Improvement by Active Steering," presented at Proceedings of the 2000 American Control Conference, Chicago, Illinois, 2000.
- [36] S.-S. You and S.-K. Jeong, "Controller design and analysis for automatic steering of passenger cars," *Mechatronics*, vol. 12, pp. 427-446, 2002.
- [37] M. Shino, Y. Wang, and M. Nagai, "Motion Control of Electric Vehicles Considering Vehicle Stability," presented at Proceedings of the 5th International Symposium on Advanced Vehicle Control (AVEC), Ann Arbor, Michigan, 2000.
- [38] K. A. Unyelioglu, C. Hatipoglu, and U. Ozguner, "Design and stability analysis of a lane following controller," *IEEE Transactions on Control Systems Technology*, vol. 5, pp. 127-134, 1997.
- [39] S. Mammari, V. B. Baghdassarian, and L. Nouveliere, "Speed Scheduled Vehicle Lateral Control," presented at Proceedings of the 1999 IEEE/IEEE/JSAI International Conference on Intelligent Transportation Systems (Cat. No.99TH8383), 1999.
- [40] G. J. Heydinger, R. A. Bixel, W. R. Garrott, M. Pyne, J. G. Howe, and D. A. Guenther, "Measured Vehicle Inertial Parameters - NHTSA's Data Through November 1998," *Society of Automotive Engineers*, 1999.
- [41] M. Mitschke, *Dynamik der Kraftfahrzeuge*, vol. A, B, C. Berlin: Springer Verlag, 1995.
- [42] J. C. Dixon, *Tires, Suspension, and Handling*, 2nd ed. Warrendale, PA: The Society of Automotive Engineers (SAE), 1996.
- [43] T. D. Gillespie, *Fundamentals of Vehicle Dynamics*: Society of Automotive Engineers (SAE), 1992.
- [44] G. J. Heydinger, W. R. Garrott, J. P. Chrstos, and D. A. Guenther, "Dynamic Effects of Tire Lag on Simulation Yaw Predictions," *Journal of Dynamic Systems, Measurement and Control, Transactions of the ASME*, vol. 116, pp. 249-256, 1994.
- [45] A. Ganguli and R. Rajamani, "Fault Diagnostic for GPS-based Lateral Vehicle Control," *Vehicle System Dynamics*, vol. 39, pp. 99-120, 2003.
- [46] B.-C. Chen and H. Peng, "A Real-time Rollover Threat Index for Sports Utility Vehicles," presented at Proceedings of the 1999 American Control Conference, San Diego, California, 1999.
- [47] B.-C. Chen and H. Peng, "Rollover Prevention for Sports Utility Vehicles with Human-In-The-Loop Evaluations," presented at Proceedings of the 5th International Symposium on Advanced Vehicle Control (AVEC), Ann Arbor, Michigan, 2000.
- [48] S. Kueperkoch, J. Ahmed, A. Kojic, and J. Hathout, "Novel Vehicle Stability Control Using Steer-by-Wire and Independent Four Wheel Torque Distribution," presented at (none), Washington, D.C, 2003.